Journal of ELECTRONIC MATERIALS, Vol. 46, No. 7, 2017
DOI: 10.1007/s11664-017-5354-7
© 2017 The Minerals, Metals & Materials Society

CrossMark

Current Analysis and Modeling of Fullerene Single-Electron Transistor at Room Temperature

VAHIDEH KHADEM HOSSEINI,[1] MOHAMMAD TAGHI AHMADI,[1,2,4,5] SAEID AFRANG,[1,3] and RAZALI ISMAIL[4]

1.—Department of Electrical Engineering, Pardis of Urmia University, Urmia, Iran. 2.—Nanotechnology Research Center, Nano Electronic Research Group, Physics Department, Urmia University, Urmia, Iran. 3.—Department of Electrical Engineering, Urmia University, Urmia, Iran. 4.—Faculty of Electrical Engineering, Universiti Teknologi Malaysia (UTM), 81310 Johor Bahru, Johor, Malaysia. 5.—e-mail: mt.Ahmadi@urmia.ac.ir

Single-electron transistors (SETs) are interesting electronic devices that have become key elements in modern nanoelectronic systems. SETs operate quickly because they use individual electrons, with the number transferred playing a key role in their switching behavior. However, rapid transmission of electrons can cause their accumulation at the island, affecting the *I–V* characteristic. Selection of fullerene as a nanoscale zero-dimensional material with high stability, and controllable size in the fabrication process, can overcome this charge accumulation issue and improve the reliability of SETs. Herein, the current in a fullerene SET is modeled and compared with experimental data for a silicon SET. Furthermore, a weaker Coulomb staircase and improved reliability are reported. Moreover, the applied gate voltage and fullerene diameter are found to be directly associated with the *I–V* curve, enabling the desired current to be achieved by controlling the fullerene diameter.

Key words: Applied gate voltage, Coulomb blocked, fullerene, island length, nanoscale, single-electron transistor

INTRODUCTION

Single-electron transistors (SETs) are Coulomb blockade (CB) devices that produce the desired current through controlled electron tunneling. The SET has two electrodes (drain and source), which are coupled to an island through tunnel junctions, while the island is also connected to the gate electrode through a capacitance C_g. This capacitance can be used to tune the electrical potential and thereby the current flow.[1–3] Electron transmission is possible in four directions, as indicated in Fig. 1, where the plus or minus sign depends on the polarity of V_{DS}.[4,5]

Electron tunneling is prevented by CB, so that electrons cannot move from the source to drain, so the conditions for CB should be explained for improved understanding. The first condition is that the initial charge on the island must be higher than the bias voltage. The second condition is that the thermal energy $K_B T$ must be lower than the charging energy. The third condition states that the tunneling resistance R_T should be more than 25,813 Ω. When the external applied voltage exceeds the Coulomb gap voltage, the Coulomb barrier is removed. The Coulomb charging energy exceeds the thermal excitation at the same temperature.[1–3] Electron transfer and the CB effect are illustrated by the energy band diagram shown in Fig. 2.

In addition, the number of electrons on the island increases with the movement of electrons across the Coulomb barrier. Therefore, the applied bias is another factor increasing electron transfer. Accumulation of charge can then occur at the island, affecting the *I–V* characteristic. The resulting Coulomb staircase behavior reduces the accuracy and reliability of the SET. Solving this limitation

(Received June 1, 2016; accepted February 3, 2017; published online February 27, 2017)

requires use of a new material with higher electron transfer rate.[6,7]

Graphene is a new carbon material explored by Andre Geim and Konstantin Novoselov in 2004, for which they won the Nobel Prize in Physics in 2010. It consists of carbon atoms arranged in honeycomb shape, and its special lattice results in unique properties such as ballistic transport, high electron mobility, and fast electron transmission. Moreover, the temperature coefficient of this material is negative, meaning that its physical properties decrease with increasing temperature. In addition, its electrical resistivity is low, so electric charges can move easily and the electrical conductivity is high, hence current flows quickly.[8–14] Due to these properties, graphene has been used for fabrication of nanoscale switches such as SETs. On the other hand, the allotrope of graphene chosen for the SET structure should be stable in the nanorange and its size controllable during fabrication. Due to its spherical shape, the aforementioned properties can be achieved by using fullerene, whose natural forms are C_{60}, C_{70}, C_{76}, C_{82}, and C_{84} molecules. The fullerene molecule (C_{60}), which is smaller than the other forms, has been investigated for use in SET islands.[15,16] The structure of a fullerene SET is shown in Fig. 3.

RESULTS AND DISCUSSION

Basic Equations for the Single-Electron Transistor

The SET consists of two serial tunnel junctions with an island between them to enable electrons to tunnel through the capacitances C_1 and C_2 after overcoming the Coulomb energy, as shown in Fig. 4.[1,2,5,17]

In the charge flow process, the system's free energy before and after electron tunneling plays a key role. The free energy of the first and second junction can be calculated respectively as

$$\Delta E_1 = \frac{e}{\sum c}\left(ne + \frac{e}{2} - V_D\left(C_2 + \frac{C_g}{2}\right) - C_g V_g\right), \quad (1)$$

$$\Delta E_2 = \frac{e}{\sum c}\left(-ne + \frac{e}{2} + V_D\left(C_2 + \frac{C_g}{2}\right) + C_g V_g\right), \quad (2)$$

where e is the electron unit charge, $\sum c$ is the sum of the drain, gate, and source capacitances, n is the number of excess electrons on the Coulomb island, and V_D and V_g are the drain and gate bias, respectively.

The single-electron tunneling rates for each junction are very important factors. Moreover, they depend on the tunneling resistance of each junction and the total energy change of the system. The tunneling probability can be expressed as follows:

$$\Gamma_j^{\pm}(N) = \frac{1}{R_j e^2}\left[\frac{-\Delta E_j^{\pm}(N)}{1 - \exp[\Delta E_j^{\pm}(N)/K_B T]}\right], \quad (3)$$

where K_B, N, and T are the Boltzmann constant, the number of electrons on the island, and the absolute temperature, respectively. R_j is the junction resistivity. Furthermore, electrons tunnel through the capacitor. The left to right direction and right to left direction correspond to the plus and minus sign, respectively. Finally, the SET current can be calculated as[18]

$$I(V) = e\sum_{N=-\infty}^{+\infty} \rho(N)\left[\Gamma_1^+(N) - \Gamma_1^-(N)\right] = e\sum_{N=-\infty}^{+\infty} \rho(N)\left[\Gamma_2^+(N) - \Gamma_2^-(N)\right]. \quad (4)$$

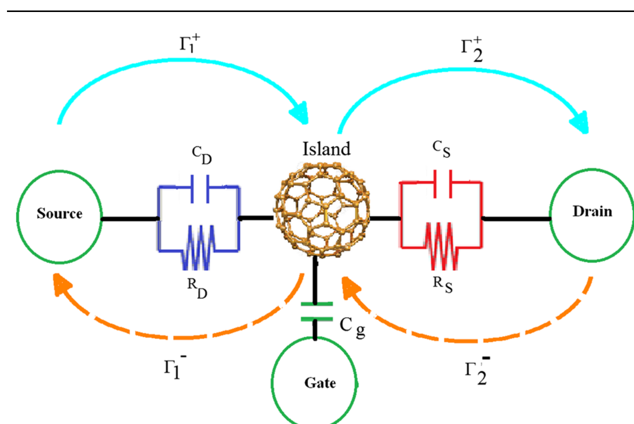

Fig. 1. Electron tunneling paths in a SET.

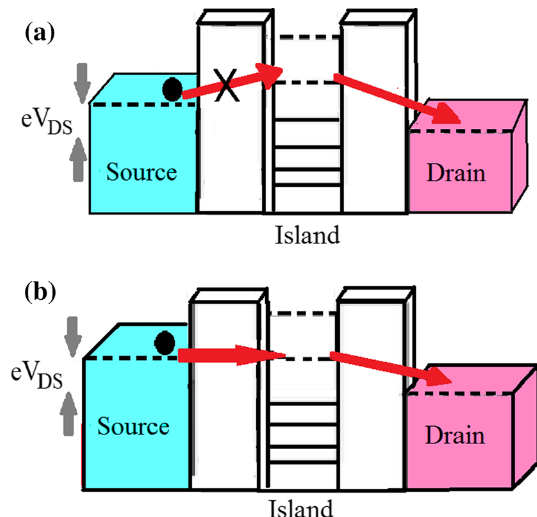

Fig. 2. (a) Coulomb-blocked condition with zero current. (b) Sufficient drain–source bias voltage for transfer across the barrier.

Current Model for the Fullerene Single-Electron Transistor

The SET can control electron tunneling to amplify the current due to quantum-mechanical effects in which the boundaries result in scattering by a one-dimensional potential barrier and tunneling. Based on the fundamentals of quantum mechanics, when a wave crosses several regions of space separated by different boundaries, the wavefunction of the first region is different from that in the second or third, while the boundary conditions specify quantities that are the same in neighboring regions. Therefore, the SET can be divided into three parts, corresponding to the drain, source, and island, as shown in Fig. 5a. The energy as a function of position along the SET channel length including the barriers is plotted in Fig. 5b, then Schrödinger's equation is written for each region.

Considering the zero potential in the left and right regions and the middle region affected by the $V(x)$ potential, Schrödinger's equation for the three parts of the fullerene SET can be written as follows:

$$-\frac{\hbar^2}{2m}\frac{\partial^2}{\partial x^2}\psi_{\mathrm{I}}(x) = E\psi_{\mathrm{I}}(x), \qquad (5)$$

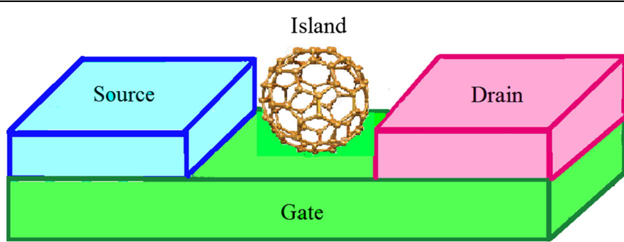

Fig. 3. SET with fullerene island.

$$\left[-\frac{\hbar^2}{2m}\frac{\partial^2}{\partial x^2} + V(x)\right]\psi_{\mathrm{II}}(x) = E\psi_{\mathrm{II}}(x), \qquad (6)$$

$$-\frac{\hbar^2}{2m}\frac{\partial^2}{\partial x^2}\psi_{\mathrm{III}}(x) = E\psi_{\mathrm{III}}(x). \qquad (7)$$

Schrödinger's equation for each region can be solved as

$$\psi_{\mathrm{I}}(x) = A_1 e^{ik_1x} + B_1 e^{-ik_1x}, \quad \text{where} \quad k_1 = \frac{\sqrt{2m(E)}}{\hbar} \qquad (8)$$

$$\psi_{\mathrm{II}}(x) = A_2 e^{k_2x} + B_2 e^{-k_2x}, \quad \text{where} \quad k_2 = \frac{\sqrt{2m(V-E)}}{\hbar}, \qquad (9)$$

$$\psi_{\mathrm{III}}(x) = A_3 e^{ik_3x}, \quad \text{where} \quad k_1 = k_3. \qquad (10)$$

The fullerene SET consists of three regions, with two electrodes that act as channels and a fullerene island which is considered to act as a barrier, extending from $x = 0$ to $x = a$. The conditions at these boundaries can be written as follows:

$$\psi_{\mathrm{I}}(0) = \psi_{\mathrm{II}}(0) \Rightarrow A_1 + B_1 = A_2 + B_2, \qquad (11)$$

$$\psi'_{\mathrm{I}}(0) = \psi'_{\mathrm{II}}(0) \Rightarrow ik_1A_1 - ik_1B_1 = k_2A_2 - k_2B_2, \qquad (12)$$

$$\psi_{\mathrm{II}}(a) = \psi_{\mathrm{III}}(a) \Rightarrow A_2e^{k_2a} + B_2e^{-k_2a} = A_3e^{-ik_1a}, \qquad (13)$$

$$\psi'_{\mathrm{II}}(a) = \psi'_{\mathrm{III}}(a) \Rightarrow k_2A_2e^{k_2a} - k_2B_2e^{-k_2a} = ik_1A_3e^{ik_1a}. \qquad (14)$$

The simplified dispersion relation between the electron energy E and wavenumber k is[19,20]

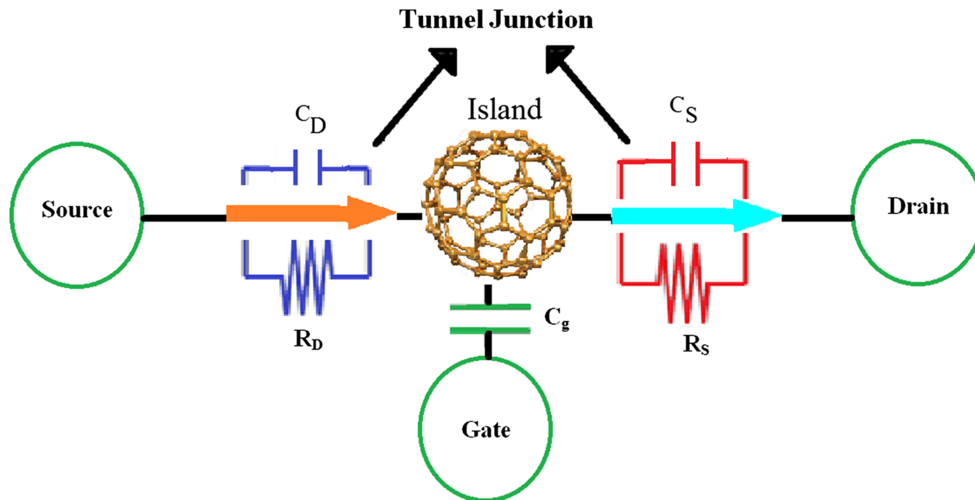

Fig. 4. Charge flow in SET circuit when an electron tunnels through capacitances C_1 and C_2.

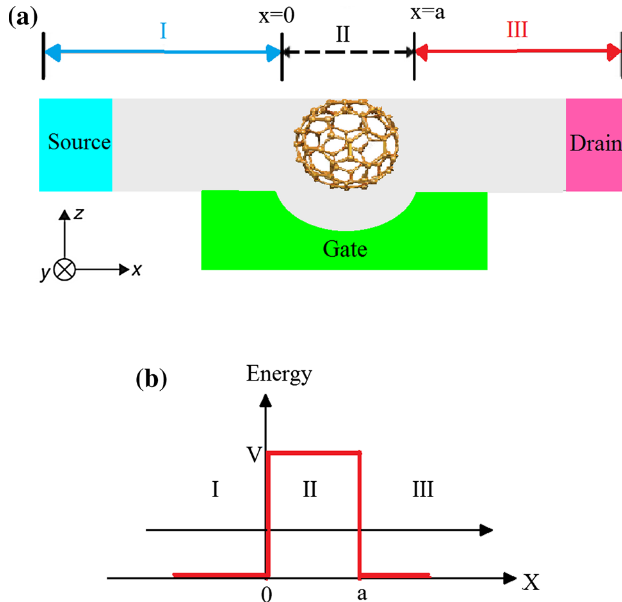

Fig. 5. (a) Schematic of SET regions. (b) SET energy versus position in channel region, indicating the junction barrier.

$$k = \left(\frac{2(E-E_0)}{ta'''}\right)^{\frac{1}{2}}. \tag{15}$$

The transmission coefficient of the fullerene SET can be calculated as

$$T = \frac{1}{1+\left(\frac{(\hbar^2+ta'''m)E-\hbar^2E_0}{2\sqrt{ta'''\hbar mE(E-E_0)}}\right)^2 \sinh^2\left(\sqrt{\frac{2mE}{\hbar^2}}a\right)}, \tag{16}$$

where E_0 is the energy bandgap of fullerene. Thus, the quantum drain current can be calculated based on the Landauer formalism as

$$I_{\rm d} = \int_0^{\eta} F(E)\cdot T(E), \tag{17}$$

where $T(E)$ is the transmission coefficient of the fullerene SET, and $F(E)$ is the Fermi probability function, i.e., the probability of occupation of energy level E, defined as

$$f(E) = \left[\frac{1}{\exp\left(\frac{E-E_{\rm F}}{K_{\rm B}T}\right)+1}\right]. \tag{18}$$

Based on this model, the current–voltage characteristic for the drain current of the fullerene SET in the parabolic-band region can be expressed as

$$I_{\rm d} = \int_0^{\eta} \frac{4c_1c_2(x+d)xK_{\rm B}T{\rm d}x}{4c_1c_2(x+d)x+(c_1(x+d)+c_2x)^2} \times \frac{1}{c_1(x+d)L^2+\frac{[c_1(x+d)L^2]^2}{3}+\frac{[c_1(x+d)L^2]^3}{36}}\cdot\frac{1}{{\rm e}^{x-\eta}+1}, \tag{19}$$

where $c_1 = 2MK_{\rm B}T/h$, $c_2 = 32MK_{\rm B}T/(9ht^2a^2_{\rm C–C})$, $d = E_{\rm g}/K_{\rm B}T$, $x = (E-E_{\rm g})/K_{\rm B}T$, and $\eta = (E_{\rm F}-E_{\rm g})/K_{\rm B}T$. Also, m is the effective mass, h is the Planck constant, $a_{\rm C–C}$ = 1.42 Å is the carbon–carbon bond length, t = 2.7 eV is the nearest-neighbor carbon–carbon tight-binding overlap energy, T is temperature, $K_{\rm B}$ is the Boltzmann constant, and L is the length of the island, which is equal to the diameter of the fullerene molecule. The suggested model depends on the fullerene diameter as

$$I_{\rm d} = \int_0^{\eta} \frac{4c_1c_2(x+d)xK_{\rm B}T{\rm d}x}{4c_1c_2(x+d)x+(c_1(x+d)+c_2x)^2} \times \frac{1}{c_1(x+d)D^2+\frac{[c_1(x+d)D^2]^2}{3}+\frac{[c_1(x+d)D^2]^3}{36}}\cdot\frac{1}{{\rm e}^{x-\eta}+1}. \tag{20}$$

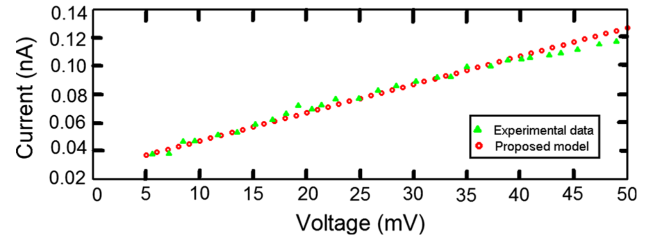

Fig. 6. Comparison of current versus voltage based on fullerene SET modeling and experimental data.

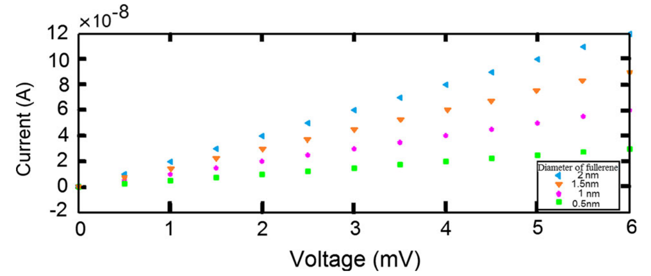

Fig. 7. I–V curves for different fullerene diameters with applied gate voltage of 1 mV.

The quantum drain current versus voltage characteristic obtained from the proposed model and experimental data from literature are plotted in Fig. 6.[21]

Comparison of these current versus voltage curves indicates acceptable agreement between the proposed model and experimental data with accuracy of 98%. The proposed model depends on the energy bands and the island length, confirming the effective role of the island material in the SET structure, as shown in Fig. 7.

The variations in Fig. 7 demonstrate the direct effect of the fullerene diameter on the current, enabling its control. Also, the applied gate voltage was investigated as a second factor, as shown in Fig. 8.

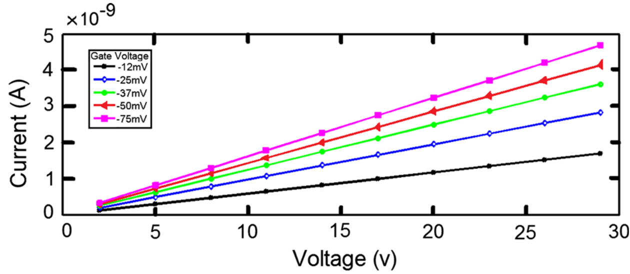

Fig. 8. *I–V* curves for different applied gate voltages with fullerene diameter of 1 nm.

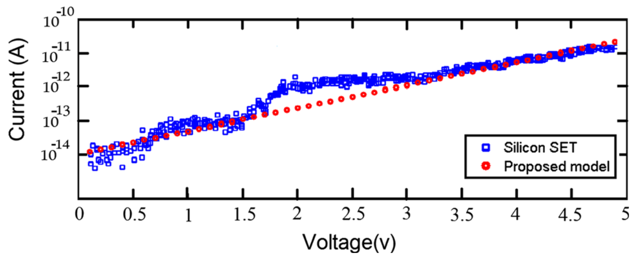

Fig. 9. Current versus drain voltage characteristic of SET; the red line shows the current of the fullerene SET at room temperature, and the blue points show the current of the silicon SET at room temperature.

Examining the changes in the *I–V* curve, the current shows a direct relation with the applied gate voltage, so by selecting a suitable gate voltage, a desired current can be achieved. Also, the current of the fullerene SET is compared with that of a silicon SET at room temperature, extracted from Fig. 9.[22]

Analysis of the *I–V* curves in Fig. 9 reveals three clear Coulomb staircase steps for the silicon SET between drain bias of 0 V and 5 V, whereas a weaker Coulomb staircase is found for the fullerene SET. This suggests that the fullerene SET will offer better accuracy and more perfect operation at room temperature. Such reliability will represent a strong reason to replace silicon transistors with fullerene transistors, enabling a rapid technology transition to nanoscale transistors based on new materials.

CONCLUSIONS

The SET is a fast electronic device for use in nanotechnology applications. It is turned on by adding an electron to the island. The increasing number of electrons on the island due to tunneling under applied bias can cause electron accumulation. Furthermore, the material used for the SET island directly impacts on its operational speed and electron transfer rate. In this work, fullerene was chosen as a zero-dimensional material for fabrication of the SET. A model is proposed for such a fullerene single-island SET, and the *I–V* characteristics plotted. Comparative analysis revealed that the fullerene SET will show weaker Coulomb staircase behavior than a silicon SET, increasing its reliability. It is hoped that fullerene SETs will replace silicon SETs in the near future. The concept of a fullerene SET with two quantum dots may also lead the way to faster switching in future technology.

REFERENCES

1. W.A. Schoonveld, J. Wildeman, D. Fichou, P.A. Bobbert, B.J. van Wees, and T. Klapwijk, *Nature* 404, 977 (2000).
2. J. Park, A.N. Pasupathy, J.I. Goldsmith, C. Chang, Y. Yaish, J.R. Petta, M. Rinkoski, J.P. Sethna, H.D. Abruña, P.L. McEuen, and D.C. Ralph, *Nature* 417, 722 (2002).
3. M. Ejrnaes, M.T. Savolainen, M.J. Manscher, and A. Mygind, *Phys. C* 372, 1353 (2002).
4. K. Likharev, *Proc. IEEE* 87, 606 (1999).
5. N. Kalhor, Ph.D. Thesis, University of Southampton, 2014, p. 26.
6. Y.A. Pashkin, Y. Nakamura, T. Yamamoto, and J.S. Tsai, *Possibility of Single-Electron Devices and Superconducting Coherence*, ed. J. Pekola, B. Ruggiero, and P. Silvestrini (New York: Springer, 2002), p. 97.
7. Y. Ono, K. Yamazaki, M. Nagas, M. Huriguchi, K. Shirashi, and Y. Takahash, *Solid State Electron.* 46, 1723 (2002).
8. A.K.N. Geim and K.S. Novoselov, *Nat. Mater.* 6, 183 (2007).
9. C. Ataca, H. Sahin, E. Akturk, and S. Ciraci, *J. Phys. Chem. C* 115, 3934 (2011).
10. F. Schwierz, *Nat. Nanotechnol.* 5, 487 (2010).
11. X. Dong, X. Zhao, L. Wang, and W. Huang, *Curr. Phys. Chem.* 3, 291 (2013).
12. T. Ragheb and Y. Massoud, in *IEEE/ACM International Conference on Computer-Aided Design* (2008), pp. 593–597.
13. E.W. Hill, A.K. Geim, K. Novoselov, F. Schedin, and P. Blake, *IEEE Trans. Magn.* 42, 2694 (2006).
14. K.S. Novoselov, A.K. Geim, S.V. Morozov, D. Jiang, Y. Zhang, S.V. Dubonos, I.V. Grigorieva, and A.A. Firsov, *Science* 306, 666 (2004).
15. O.A. Shenderova, V.V. Zhirnov, and D.W. Brenner, *Crit. Rev. Solid State Mater. Sci.* 27, 227 (2002).
16. X. Wang, Q. Li, J. Xie, Z. Jin, J. Wang, Y. Li, K. Jiang, and S. Fan, *Nano Lett.* 9, 3137 (2009).
17. J.R. Tucker, *J. Appl. Phys.* 72, 14 (1992).
18. L. Sheela, N.B. Balamurugan, S. Sudha, and J. Jasmine, *JEET* 9, 1670 (2014).
19. G.W. Semenoff, *Phys. Rev. Lett.* 53, 2449 (1984).
20. P.R. Wallace, *Phys. Rev.* 71, 622 (1947).
21. H. Park, J. Park, A.K.L. Lim, E.H. Anderson, A.P. Alivisatos, and P.L. McEuen, *Nature* 407, 57 (2000).
22. A.Z. Khan Durrani, *Single-Electron Devices and Circuits in Silicon* (London: Imperial College Press, 2010), p. 127.